On Antenna Mounting Position for 6G Vehicular Communications

Marouan Mizmizi[#1], Dario Tagliaferri[#2], Monica Nicoli[*3], Umberto Spagnolini[#4]
[#]Dipartimento di Elettronica, Informazione e Bioingegneria (DEIB), Politecnico di Milano, Milan, Italy
[*]Dipartimento di Ingegneria Gestionale (DIG), Politecnico di Milano, Milan, Italy
{[1]marouan.mizmizi, [2]dario.tagliaferri, [3]monica.nicoli, [4]umberto.spagnolini}@polimi.it

***Abstract*— Over the recent past, vehicle-to-everything (V2X) communication technology is experiencing a shift toward millimeter-wave (mmWave) and sub-THz frequencies in pursuit of more bandwidth to accommodate the requirements of future V2X services. At mmWave/sub-THz, antenna arrays and beamforming techniques must be used to overcome the higher propagation attenuation. However, the beams must be collimated, and beam management must ensure beam alignment in mobility and address beam blockage. A relevant question often ignored, which can impact communication performance, is where to place the antenna on the vehicle. This paper addresses this important issue by evaluating the impact of the antenna position (rooftop or bumper) based on blockage probability and beamforming gain loss due to road-induced vibrations affecting the beam alignment. The numerical and analytical results suggest placing the antenna on the rooftop of the vehicles, as it is more robust against both vibrations and beam blockage.**

***Keywords*— V2X communication, blockage, millimeter-waves, antenna position**

I. Introduction

The upcoming sixth-generation (6G) vehicle-to-everything (V2X) communications have been envisioned as key enablers for many emerging services with high-quality wireless connectivity requirements [1]. Among the visionary speculations about what 6G will be, the most common is to explore high frequencies, shifting from the current sub-6GHz band to millimeter-wave (mmWave) and sub-THz bands [2], where the large bandwidth available can accommodate the requirements of future V2X applications and services. The radio propagation at these frequencies is subject to additional orders of magnitude of path and penetration losses compared to currently deployed systems, calling for collimated communication and beamforming technology as a viable solution to increase the communication range. Beam management methods are needed to ensure beam alignment, also in mobility, e.g., through tracking. Recently, beam management attracted significant interest in scientific and industrial communities [3], [4], focusing on efficient solutions to limit overhead e delay introduced during beam alignment. However, beam blockage, which in high-mobility vehicular scenarios leads to frequent link failures and severely affects beam management performances, is still an open problem. Besides, as the frequency increases, e.g., sub-THz (>100GHz), with consequently narrower beamwidths, frequent link drops occur even due to vibrations caused by poor road conditions or road bumps [5]. Several studies were performed to investigate (and possibly mitigate) the impact of blockage and beam-misalignment due to vibrations on V2X communications. At 30 GHz, blockage from a vehicle causes a power loss ranging from 10 to 20 dB [6], depending on the transmitting vehicle (Tx) and receiving vehicle (Rx) position, and it increases by $5.5 - 17$ dB when multiple vehicles are simultaneously blocking the LoS. Similar results were observed experimentally in [7] by the third generation partnership project (3GPP). In [8], the authors derived the analytical blockage probability and the related SNR distribution in the case of multiple vehicles simultaneously blocking the line-of-sight in a highway vehicle-to-vehicle (V2V) scenario. The impact of road-induced vibrations on beam-based communication is still unexplored. The authors in [9] studied these effects on Doppler spread and channel estimation. The study in [10] investigates the impact of antenna vibration during the vehicle's mobility in a vehicle-to-infrastructure (V2I) scenario. The results show that loss due to beam misalignment increases for narrower beams, shorter Tx-Rx distance, or for a lower height of the base station. Current literature tackles these issues from the signal processing or network perspective. For example, the authors in [11] propose to use inertial sensors onboard the vehicle to estimate vibrations and adapt the beamwidth accordingly. In [12], vehicles cooperate to augment the collective perception of the environment, predicting possible blockers and appropriately selecting relays to bypass possible blockage events.

On the contrary, this paper aims to address the problem from a different perspective. Specifically, we investigate the impact of blockage and road-induced vibration on the antenna, considering two candidate mounting positions, i.e., bumper and rooftop levels. The work proposed here is not intended as an alternative to the aforementioned literature, but rather as a complementary approach to increase beam management robustness.

The remainder of this paper is organized as follows: Section II details the derivation of the analytical blockage probability. The road-induced vibration model is discussed in Section III, while Section IV shows the numerical results. Finally, closing remarks are discussed in Section V.

II. Blockage Modeling in V2V

The considered scenario is a single-lane road segment with a Tx and Rx vehicle and a possible blocker randomly distributed with density ρ [veh/m], as depicted in Fig. 1. Tx and Rx are equipped with a mmWave/sub-THz array of antennas

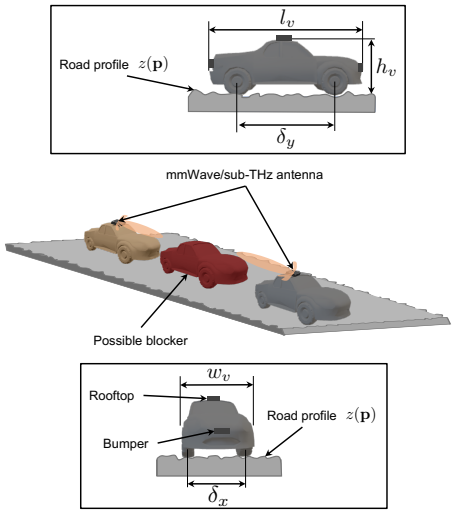

Fig. 1. Scenario and system architecture.

mounted either on the rooftop or the frontal/rear bumper as recommended by 3GPP [13]. Moreover, vehicles are assumed to have a box-shaped occupation of size $w_v \times l_v \times h_v$.

From the electromagnetic perspective, the LoS is blocked when one (or more) vehicle penetrates the first Fresnel ellipsoid, as depicted in Fig. 2. Let us assume the vehicle's height as $h_v \sim \mathcal{N}(\mu_v, \sigma_v^2)$ [14] and a single-vehicle $\mathcal{B}$ at distance d_{tb} from Tx and d_{br} from Rx. The effective height of the first Fresnel ellipsoid at the position of the blocking vehicle is

$$\tilde{h} = (h_r - h_t)\frac{d_{tb}}{d_{tr}} + h_t - 0.6\,\tilde{r} \tag{1}$$

where h_t and h_r are the heights of the Tx and Rx array of antennas, respectively and $\tilde{r}$ is the radius of the first Fresnel ellipsoid at relative distance d_{tb} and d_{br}, that is

$$\tilde{r} = \sqrt{\lambda_c \frac{d_{tb} d_{br}}{d_{tb} + d_{br}}}. \tag{2}$$

with λ_c being the carrier wavelength. Assuming the independence between the Tx and Rx heights, the Fresnel ellipsoid height is

$$\tilde{h} = h_r \frac{d_{tb}}{d_{tr}} + h_t \frac{d_{br}}{d_{tr}} - 0.6\,\tilde{r} \sim \mathcal{N}\left(\tilde{\mu}, \tilde{\sigma}^2\right) \tag{3}$$

with mean $\tilde{\mu} = \mu_v - 0.6\,\tilde{r}$ and variance $\tilde{\sigma}^2 = \sigma_v^2$. Hence, the blockage occurs when the blocking vehicle height $h_b \sim \mathcal{N}(\mu_b, \sigma_b^2)$ is larger than $\tilde{h}$, i.e., $h_{eff} = h_b - \tilde{h} > 0$. The probability of blockage conditional to the presence of a vehicle $\mathcal{B}$ between the Tx and Rx can be computed as:

$$\mathbb{P}\left(\text{NLoSv}|d_{tr}, \mathcal{B}\right) = Q\left(\frac{h_{eff} - \mu_{eff}}{\sigma_{eff}}\right) \tag{4}$$

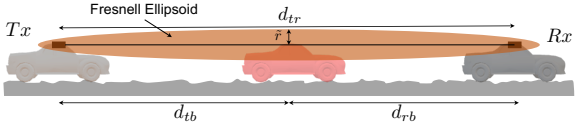

Fig. 2. Example of obstruction in the first Fresnel ellipsoid.

where $\mu_{eff} = \mu_b - \tilde{\mu}$, $\sigma_{eff}^2 = \sigma_b^2 + \tilde{\sigma}^2$, and $Q(x)$ is the Gaussian Q-function.

To derive the unconditional blockage probability, we propose to divide the distance d_{tr} between Tx and Rx into slots of length $l_s = l_v + d_s$, where l_v is the vehicle's length, and d_s accounts for safety distance between vehicles. Each slot can be occupied by one single vehicle, and the blockage occurs if one (or more) slots are occupied by a blocking vehicle. The probability that an arbitrary slot is occupied depends on the distribution of vehicles and on the length of the slot l_s. Assuming the vehicles are distributed according to a point Poisson process (PPP) as in [15], the probability that an arbitrary slot is occupied is

$$\mathbb{P}(\mathcal{B}) = \rho l_s\, e^{-\rho l_s}. \tag{5}$$

The probability that an arbitrary slot is occupied by a vehicle and that vehicle is blocking the LoS can be computed using Bayes equation

$$\mathcal{P}_s = \mathbb{P}\left(\text{NLoSv}|d_s, \mathcal{B}\right)\mathbb{P}\left(\mathcal{B}\right) = Q\left(\frac{h_{eff} - \mu_{eff}}{\sigma_{eff}}\right)\mathbb{P}(\mathcal{B}). \tag{6}$$

Finally, the unconstrained probability of blockage can be written as

$$\mathbb{P}\left(\text{NLoSv}|d_{tr}\right) = \sum_{k=1}^{N_s} \mathbb{P}\left(\text{NLoSv}^{(k)}|d_{tr}\right) \tag{7}$$

where $N_s = \lfloor d_{tr}/d_s \rfloor$ is the total number of slots and $\mathbb{P}\left(\text{NLoSv}^{(k)}|d_{tr}\right)$ is the probability of having k slots simultaneously occupied by blocking vehicles, which is given by the Bernoulli probability

$$\mathbb{P}\left(\text{NLoSv}^{(k)}|d_{tr}\right) = \binom{N_s}{k} \mathcal{P}_s^k (1 - \mathcal{P}_s)^{N_s - k}. \tag{8}$$

III. Antenna Array Vibration Modeling

Road roughness and irregularities generate high-frequency vibrations on the vehicle chassis and, consequently, on the antenna. The road profile defines how the vibrations are transferred to the chassis through the suspensions. In particular, we focus on longitudinal road profile $z(\mathbf{p})$, which is described by the displacement along the z-axis for an arbitrary position $\mathbf{p} = (x, y)$. The road profile is transferred to the suspension through direct contact with the vehicle's four wheels, as shown in Fig. 1. Considering the left-right wheel located in $\mathbf{p}_o = (x_o, y_o)$ as reference, we can obtain the road profile experienced by each wheel as $\mathbf{z} = \{z(\mathbf{p}_o), (\mathbf{p}_o + (0, \delta_y)), z(\mathbf{p}_o + (\delta_x, 0)), z(\mathbf{p}_o + (\delta_x, \delta_y))\}$, where δ_x and δ_y are the displacement between right-left and back-front wheels, respectively. According to the standard ISO 8608 [16], $z(\mathbf{p})$ can be modeled as a correlated Gaussian random process with a standard deviation that depends on the roughness of the road and the speed of the vehicle. The standard defines five road classes, ranging from low (class A) to high (class E) roughness. For example, highways are class A, while unpaved roads are class E. The detailed road profile model is in [17].

To obtain the vibration at the antenna, we first need to model the suspension transfer function. In this regard, we consider the quarter car model in [18], where the suspensions are modeled as low pass filters with a cut-off frequency f_c and a damping ratio ϵ, that are

$$f_c = \frac{1}{2\pi}\sqrt{\frac{4s}{M}}, \quad \epsilon = \frac{c_d}{2}\sqrt{\frac{4}{Ms}}, \tag{9}$$

where M is vehicle mass, s is the suspension stiffness, and c_d is damping coefficient.

Let us assume the vehicle's chassis as a rigid body [18], [19] with an instantaneous attitude defined by the ϕ, pitch ψ, and yaw θ. The filtered road profiles $z_f(\mathbf{p})$ induce a variation in roll δ_ϕ and pitch δ_ψ angles, which is derived as

$$\delta_\phi = \text{atan}\left(\left(z_f(\mathbf{p_o}) - z_f(\mathbf{p_o} + (0, \delta_y))\right)/\delta_y\right). \tag{10}$$

$$\delta_\psi = \text{atan}\left(\left(z_f(\mathbf{p_o}) - z_f(\mathbf{p_o} + (\delta_x, 0))\right)/\delta_x\right) - \tag{11}$$

Note that the yaw θ is only affected by the driving behavior (inputs from the steering wheel) and not by the road profile. The variations in (10) cause beam misalignments and, consequently, beamforming gain loss. Assuming both Tx and Rx are equipped with the same antenna array, the total beamforming gain can be expressed as

$$G_{\text{total}} = G_t \times G_r = G_o^2 A(\hat{\vartheta}_t, \hat{\varphi}_t) A(\hat{\vartheta}_r, \hat{\varphi}_r)) \tag{12}$$

where G_o is the maximum beamforming gain, $A(\hat{\vartheta}, \hat{\varphi}) \leq 1$ s the array directivity function, and $\hat{\vartheta}$ and $\hat{\varphi}$ are the azimuth and elevation pointing directions, respectively. Notice that by assuming perfect beam alignment and no attitude variations lead to no gain-loss, i.e., $A(\hat{\vartheta}, \hat{\varphi}) = 1$, for all the other cases, the system will experience a gain-loss $A(\hat{\vartheta}, \hat{\varphi}) < 1$.

IV. Numerical Simulations

This section presents the numerical results of the proposed analytical framework. In particular, we analyze the blockage probability and the beamforming gain-loss induced by vibrations considering the antenna array mounted at the bumper and rooftop levels, as depicted in Fig. 1. The beamforming gain-loss is computed, based on (12), in dB scale as

$$G_{\text{Loss}} = A(\hat{\vartheta}_t, \hat{\varphi}_t) + A(\hat{\vartheta}_r, \hat{\varphi}_r) \tag{13}$$

where the pointing angles $(\hat{\vartheta}, \hat{\varphi})$ are only affected by the roll δ_ψ and pitch δ_{phi} variations in (10). Both Tx and Rx are equipped with a squared uniform planar array (UPA) with $N_a \times N_a$ elements. Unless otherwise specified, the simulation parameters in Table 1 are used. These parameters are selected based on the 3GPP recommendation in [13] and ISO [16].

The analytical blockage probability model here derived is validated through extensive Monte Carlo simulations, as can be observed in Fig. 3 (a) and (b). More specifically, Fig. 3 (a) depicts the blockage probability varying the vehicle density ρ and considering two reference Tx-Rx distances, namely $d_{tr} = 50$ and $d_{tr} = 150$ m. The blue curve shows the blockage probability when the antenna is mounted on the vehicle's rooftop, while in the red curve, the antenna is mounted on the vehicle's bumper. Both curves increase with the vehicle density ρ, and for the shortest distance, we observe the highest gap between rooftop and bumper mounting positions. For large distances, the gap between the two curves reduces considerably, as the first Fresnel ellipsoid radius becomes larger and the probability of obstruction increases. The blockage probability varying the Tx-Rx distance d_{tr} is depicted in Fig. 3 (b), considering two reference vehicle densities, namely $\rho = 10$ and $\rho = 50$ [veh/km]. Likewise, in this case, both curves increase with the Tx-Rx distance d_{tr}. The gap for rooftop and bumper mounting positions, in both cases, is approximately constant at around 10%. The increase of blockage probability with the distance is due to the larger first Fresnel ellipsoid radius. The impact of the road-induced vibrations on the beam pointing can be observed in Fig. 4, considering two UPA configuration: $N_a = 16$ and

Table 1. Simulation Parameters

Parameter	Symbol	Value
Vehicle length, width	$[l_v, w_v]$	$[5, 1.8]$ m
Vehicle wheels displacement	$[\delta_y, \delta_x]$	$[3.5, 1.5]$ m
Vehicle height mean and std. dev.	$\mu_{h,v}, \sigma_{h,v}$	$[1.5, 0.08]$ m
Vehicle Mass	M	1300 Kg
Vehicle Speed	V	50 Km/h
Suspension cut-off frequency	f_c	1 Hz
Suspension damping rate	ϵ	0.2
Inter-vehicle safety distance	d_s	2.5 m

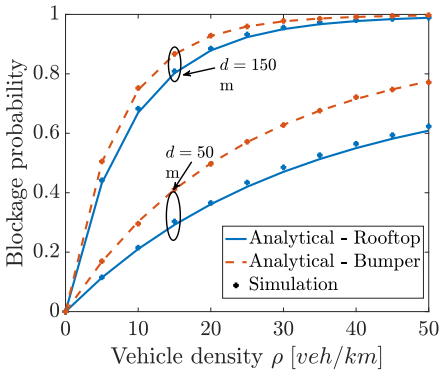

(a)

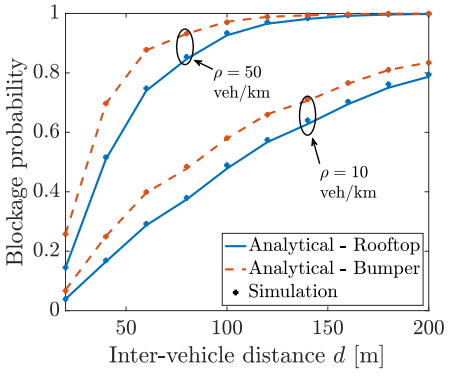

(b)

Fig. 3. Analytical and simulated blockage probability: (a) varying the vehicle density ρ, considering two reference distances 50 and 150 m, and (b) varying the Tx-Rx distance, considering two reference vehicle densities, 10 and 50 [veh/km].

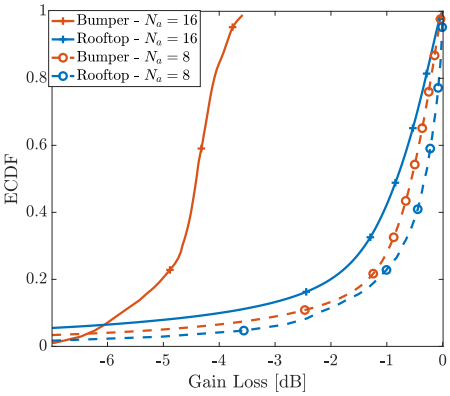

Fig. 4. Empirical cumulative distribution function of the beamforming gain-loss.

$N_a = 8$ elements with a beamwidth of 6 deg and 12 deg, respectively.The road profile considered in this simulation is based on the class E pavement parameters in [16]. The road-induced vibration causes a significant beamforming gain-loss when beamwidth decreases, and the impact is more evident when the array of antennas is mounted on the bumper. This behavior is due to the stronger vibrations transmitted to the bumper compared to the rooftop position, as it is located more distant from the vehicle's center of gravity. The analysis presented in this paper suggests that the array of antennas for mmWave/sub-THz communication should be mounted on the rooftop of vehicles, as it reduces the probability of blockage and reduces the effect of road vibrations on the beam pointing accuracy. Besides the blockage and vibration issues, the array of antennas located on the bumper is more prone to damage than the rooftop due to more likely rear-end collisions with other vehicles. These results can be valuable in designing solutions that increase the reliability and robustness of future V2X networks.

V. Conclusion

The usage of narrow beams to compensate for the increased path and penetration loss at mmWave/sub-THz frequency bands make the beam and blockage management the main challenges for seamless and robust V2X communications. More specifically, frequent link outages occur caused by random blockage from non-connected vehicles and, to a minor extent, beam misalignment due to road-induced vibrations. In this setting, this paper addresses the issue of determining the optimal mounting position for the mmWave/sub-THz antenna array on-board a vehicle, namely rooftop and bumper, analyzing the blockage probability and the road-induced beamforming gain loss in a realistic vehicular scenario. The simulation results indicate the rooftop as the best antenna placement, whereas bumper mounting suffers from higher blockage probability and gain loss.

Acknowledgment

The work has been partially carried out within the joint research lab between Huawei and Politecnico di Milano.

References

[1] Z. Zhang, Y. Xiao, Z. Ma, M. Xiao, Z. Ding, X. Lei, G. K. Karagiannidis, and P. Fan, "6g wireless networks: Vision, requirements, architecture, and key technologies," *IEEE Vehicular Technology Magazine*, vol. 14, no. 3, pp. 28–41, 2019.

[2] F. Tariq, M. R. A. Khandaker, K.-K. Wong, M. A. Imran, M. Bennis, and M. Debbah, "A speculative study on 6g," *IEEE Wireless Communications*, vol. 27, no. 4, pp. 118–125, 2020.

[3] T. Shimizu, V. Va, G. Bansal, and R. W. Heath, "Millimeter wave v2x communications: Use cases and design considerations of beam management," in *2018 Asia-Pacific Microwave Conference (APMC)*, 2018, pp. 183–185.

[4] M. Mizmizi, F. Linsalata, M. Brambilla, F. Morandi, K. Dong, M. Magarini, M. Nicoli, M. N. Khormuji, P. Wang, R. A. Pitaval *et al.*, "Fastening the initial access in 5g nr sidelink for 6g v2x networks," *Vehicular Communications*, vol. 33, p. 100402, 2022.

[5] C. K. Anjinappa and I. Guvenc, "Millimeter-wave v2x channels: Propagation statistics, beamforming, and blockage," in *2018 IEEE 88th Vehicular Technology Conference (VTC-Fall)*, 2018, pp. 1–6.

[6] J.-J. Park, J. Lee, J. Liang, K.-W. Kim, K.-c. Lee, and M.-D. Kim, "Millimeter wave vehicular blockage characteristics based on 28 GHz measurements," in *2017 IEEE 86th Vehicular Technology Conference (VTC-Fall)*. IEEE, 2017, pp. 1–5.

[7] G. T. R. W. M. 93, "V2X sidelink channel model," vol. R1-1807672, May 2017.

[8] K. Dong, M. Mizmizi, D. Tagliaferri, and U. Spagnolini, "Vehicular blockage modelling and performance analysis for mmwave v2v communications," *arXiv preprint arXiv:2110.10576*, 2021.

[9] J. Blumenstein, J. Vychodil, M. Pospisil, T. Mikulasek, and A. Prokes, "Effects of vehicle vibrations on mm-wave channel: Doppler spread and correlative channel sounding," in *2016 IEEE 27th Annual International Symposium on Personal, Indoor, and Mobile Radio Communications (PIMRC)*. IEEE, 2016, pp. 1–5.

[10] K. A. Al Mallak, M. Nair, G. Hilton, T. H. Loh, and M. Beach, "Characterising vehicle suspension variations in millimetre wave v2i system," in *2021 IEEE 93rd Vehicular Technology Conference (VTC2021-Spring)*. IEEE, 2021, pp. 1–5.

[11] D. Tagliaferri, M. Brambilla, M. Nicoli, and U. Spagnolini, "Sensor-aided beamwidth and power control for next generation vehicular communications," *IEEE Access*, vol. 9, pp. 56 301–56 317, 2021.

[12] F. Linsalata, S. Mura, M. Mizmizi, M. Magarini, P. Wang, M. N. Khormuji, A. Perotti, and U. Spagnolini, "Los-map construction for proactive relay of opportunity selection in 6g v2x systems," *arXiv preprint arXiv:2111.07804*, 2021.

[13] 3rd Generation Partnership Project (3GPP), "Study on evaluation methodology of new vehicle-to-everything (V2X) use cases for LTE and NR (TR 37.885)," 2019.06.

[14] N. Akhtar, S. C. Ergen, and O. Ozkasap, "Vehicle mobility and communication channel models for realistic and efficient highway vanet simulation," *IEEE Transactions on Vehicular Technology*, vol. 64, no. 1, pp. 248–262, 2014.

[15] A. Abul-Magd, "Modeling highway-traffic headway distributions using superstatistics," *Physical Review E*, vol. 76, no. 5, p. 057101, 2007.

[16] I. 8608, "Mechanical vibration - road surface profile - reporting of measured data," 2016.

[17] P. Johannesson, K. Podgórski, and I. Rychlik, "Modelling roughness of road profiles on parallel tracks using roughness indicators," *International journal of vehicle design*, vol. 70, no. 2, pp. 183–210, 2016.

[18] S. M. Savaresi, C. Poussot-Vassal, C. Spelta, O. Sename, and L. Dugard, *Semi-active suspension control design for vehicles*. Elsevier, 2010.

[19] G. Ciaramitaro, M. Brambilla, D. Tagliaferri, E. Bozzi, M. Nicoli, A. Perotti, and U. Spagnolini, "On the impact of road roughness and antenna position on vehicular communications," *IEEE Wireless Communications Letters*, pp. 1–1, 2022.